Reprint

Multipath Characterization of Indoor Power Line Networks

D. Anastasiadou and Th. Antonakopoulos

IEEE Transactions on Power Delivery

VOL. 20, NO. 1, JANUARY 2005, pp. 90 - 99

Multipath Characterization of Indoor Power-Line Networks

Despina Anastasiadou and Theodore Antonakopoulos, *Senior Member, IEEE*

***Abstract*—The time- and frequency-varying behavior of an indoor power-line network is the result of variable impedance loads connected to its termination points. In fact, any signal transmitted through such a communications network is subject to time-varying multipath fading. In this paper, an analytical calculation method is presented, which can be used to determine the multipath components of any point-to-point channel in the indoor power-line environment. The method calculates all transmission characteristics of the network and, therefore, it can be exploited in the process of designing proper transmission algorithms for optimizing system performance. The proposed method is applied to an example network to demonstrate its usefulness in explaining the network's time-dependent behavior and in estimating channel parameters, such as subchannel bandwidth, multipath delay spread, fading conditions, etc.**

***Index Terms*—Delay effects, multipath channels, power transmission lines, time-varying channels.**

I. Introduction

THE increasing demand for broadband telecommunication services in today's small-office/home-office (SOHO) environment has aroused an interest in the exploitation of alternative communications media [1]. The indoor power grid is a prominent candidate, with its main advantages resulting from the utilization of the existing infrastructure and the abundance of access points, in the form of ac outlets. However, the development of viable power-line systems for providing telecommunication services requires statistical modeling of the channel's time-varying behavior based on analytical and experimental results.

The power-line channel differs considerably in topology, structure, and physical properties from conventional media such as twisted pair, coaxial, and fiber-optical cables, exhibiting rather hostile characteristics. Initially designed solely for power distribution, the power grid is far from being optimized for high-speed data transmission. Common causes of impairment include time- and frequency-varying impedances and considerable noise due to loads connected to its outlets. As a result, variable levels of signal attenuation are observed on the channel [2]. Various measurement-based and analytical models have been proposed in the literature, concerning the communications properties of the indoor power grid. The most common approach considers the channel as a "black box" and extracts a number of system parameters using extensive experimental results [3]. Using the same approach, the channel has been examined as a multipath environment, whose characteristics can be determined using experimental measurements [4]. Statistical modeling of the measured additive noise [5] and derivation of the channel's transfer function have also been attempted. Nevertheless, a widely accepted channel model has not yet been presented, since models based on experimental results, obtained on specific topologies and under certain conditions, fail to offer a generally applicable description of the power-line network behavior.

Modeling the power line for high-speed communications can be aided by analyzing the multipath nature of the power grid, arising from the presence of several branches and impedance mismatches, which cause numerous reflections of the transmitted signal. In this paper, we present an algorithm that performs analytical calculation of the multipath effect between any pair of communicating devices on the indoor power-line network by tracing it back to its physical characteristics, such as cable loss, reflection, and transmission coefficients. Analytical calculation of the multipath components in the indoor power grid is feasible due to its loop-free topology and its bounded complexity, thus making it possible to predict the response of any point-to-point channel, based on information about the network's physical structure, topology, and termination loading. Modeling the power-line channel as a multipath environment is needed in order to determine the transmission paths that contribute to its time- and frequency-variable behavior and to calculate the parameters that define the medium's communications properties, such as the root mean square (rms) delay spread, which indirectly determines the achievable data transmission rate.

The paper is organized as follows: Section II describes multipath propagation through the power-line channel and associates its response to the network's physical characteristics. The algorithm used to perform analytical calculation of the multipath signal components is presented in Section III. Finally, Section IV demonstrates the algorithm's usefulness in estimating important communications parameters by presenting typical results obtained for an example network.

II. Transmission in the Indoor Power-Line Environment

The variety of loads connected to the network's termination points (ac outlets) and the presence of several cable branches result in impedance mismatches that cause multipath signal propagation in the indoor power-line environment. Even in a homo-

Manuscript received August 18, 2003. Paper no. TPWRD-00430-2003. This work was supported in part by the "Karatheodoris" R&D program of the University of Patras. This paper was presented in part at the IEEE International Symposium on Circuits and Systems–ISCAS 2003, Bangkok, Thailand, May 2003.

The authors are with the Department of Electrical Engineering and Computer Technology, University of Patras, Patras 26500, Greece (e-mail: desan@loe.ee.upatras.gr; antonako@ee.upatras.gr).

Digital Object Identifier 10.1109/TPWRD.2004.832373

geneous network constructed using a single type of cable, the traveling signal suffers a reflection at every point of impedance mismatch, caused by the difference between the cable's characteristic impedance and the termination impedance or even by the parallel connection of a number of cables at a network junction point. As a result, part of the arriving signal is reflected back toward its origin, while the remaining signal proceeds in the initial direction. Thus, for a cable with characteristic impedance Z_0, the reflection coefficient ρ at a certain discontinuity, where an impedance of Z_L is connected, expresses the amplitude and phase ratio of the backward propagating (reflected) signal to the originally arriving signal. The corresponding transmission coefficient τ expresses the analogous for the forward propagating signal. These coefficients are calculated using the following expressions:

$$\rho = \frac{Z_L - Z_0}{Z_L + Z_0} \quad \text{and} \quad \tau = 1 + \rho = \frac{2Z_L}{Z_L + Z_0}. \tag{1}$$

Considering a theoretically infinite number of reflections inside the power-line network, we can deduce that the received signal is composed of infinite distorted replicas of the initially transmitted signal, commonly referred to as multipath components, which differ both in amplitude and phase. Each component represents the result of propagation through a particular path, since its amplitude and phase (or delay) depend on the path's length and the reflection and transmission coefficients that comprise it. However, from a more practical point of view, as the length of a path increases, more reflections occur, the attenuation level rises, and, therefore, the path's contribution to the overall received signal decreases. As a result, the multipath effect can be bounded to a finite number of significant paths. Moreover, unlike in the case of a wireless environment, analytical calculation of the multipath effect in an indoor power-line network is feasible, since its topology is relatively limited in complexity and does not contain loops. Therefore, the response between any pair of communicating devices on the network can be determined using information about the cable's transmission properties, the network's topology, and the impedances connected to its outlets.

Transmission between the two network termination points that define the communications channel is done through a large number of paths. Each path is characterized by a propagation loss factor, a reflection factor, and a delay. The propagation loss factor (g_i) and the delay (τ_{di}) of the ith path depend on its length and the physical characteristics of the cable, according to the following expressions:

$$g_i = e^{-\alpha l_i} \tag{2}$$

$$\tau_{di} = \frac{l_i}{v} = \frac{l_i}{\omega/\beta} \tag{3}$$

where l_i is the path's length, v is the group velocity of propagation, and $\gamma = \alpha + j\beta$ is the propagation constant of the line, defined by the attenuation constant α and the phase constant β.

The reflection factor of a particular path is the product of all reflection or transmission coefficients that comprise it. The following expression corresponds to the total reflection factor

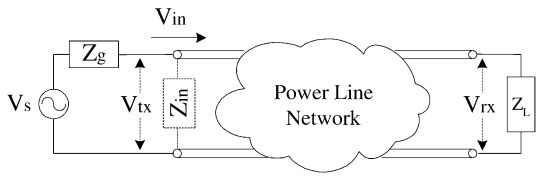

Fig. 1. Point-to-point channel on a power-line network.

$(r_i e^{j\theta_i})$ of the ith path, which consists of M not necessarily different discontinuities:

$$r_i e^{j\theta_i} = \prod_{k=1}^{M_1} \{\rho_{ik}\} \prod_{n=1}^{M_2} \{\tau_{in}\}, \quad \text{where } M_1 + M_2 = M. \tag{4}$$

Indices k and n indicate each of the M_1 and M_2 discontinuities included in path i.

We calculate the channel's complex impulse response, namely its delay-spread function, based on the general multipath propagation equations. Considering that transmission of an impulse $\delta(t)$ through a multipath environment with L paths results in a train of delayed impulses, we modify the general expression to suit the case of an indoor power-line communications network. Thus, the channel's impulse response can be calculated as the sum of all multipath components according to

$$h(\tau_d, t) = \sum_{i=1}^{L} \left\{ r_i e^{j\theta_i} \cdot e^{-\alpha l_i} \cdot \delta\left(t - \tau_{di}\right) \right\}. \tag{5}$$

Taking (3) into consideration, the equivalent frequency response function is given by

$$\begin{aligned} H(f) &= \sum_{i=1}^{L} \{ r_i e^{j\theta_i} \cdot e^{-\alpha l_i} \cdot e^{-j\omega\tau_{di}} \} \\ &= \sum_{i=1}^{L} \{ r_i e^{j\theta_i} \cdot e^{-\gamma l_i} \}. \end{aligned} \tag{6}$$

The above expression is the frequency-domain ratio of the channel's output voltage (V_{rx}) to the voltage injected into the line (V_{in}) by an ideal generator $(Z_g = 0)$. In the case of a practical power-line network, as shown in Fig. 1, calculation of the transfer function between any two communicating devices involves an additional scaling factor, which includes the nonideal characteristics of the transmission system. Since the transfer function of a point-to-point channel represents the ratio of the steady state voltages measured at the two communicating ends, another scaling factor has to be added, relating the incoming source voltage (V_s) to the total voltage measured at the transmission end (V_{tx}), which comprises the injected signal and the sum of all signal components that are reflected toward the source. Calculation of the above scaling factors is performed by applying Kirchhoff's laws. As a result, we derive the following expression for the transfer function of the channel, which is calculated as the ratio of the voltages measured at the two communicating termination points:

$$T(f) = \frac{V_{rx}}{V_{tx}} = \frac{Z_0}{Z_0 + Z_g} \cdot \frac{Z_{\text{in}} + Z_g}{Z_{\text{in}}} \cdot \sum_{i=1}^{L} \{ r_i e^{j\theta_i} \cdot e^{-\gamma l_i} \} \tag{7}$$

where Z_{in} is the input impedance appearing at the transmission end in steady state.

III. Multipath Components' Calculation Algorithm

In order to estimate the transfer function between two communicating devices on the network, we developed an algorithm that analytically calculates the multipath channel components. The algorithm uses a set of network description matrices, specifically defined to include all of the necessary information about the network's physical characteristics, topology, and termination impedances. The algorithm performs the calculation of every reflection and transmission coefficient on the network, along with the input impedances appearing at every network termination. The algorithm identifies a large number of possible signal paths $L_{\max}$ inside the network and calculates the respective lengths, total reflection and propagation factors. It proceeds to select the L most significant transmission paths, based on their contribution to the overall output signal power, where $L \ll L_{\max}$ is based on their contribution to the overall output signal power.

The algorithm's flexibility is based on a general calculation procedure that uses a set of network description matrices that represent any network topology along with its loading conditions. Additionally, the algorithm takes into consideration the following conditions, which are always valid in the indoor power-line environment.

- Each termination point is connected to a single node.
- Direct connections between termination points do not exist.
- No loops exist since the network has radial topology.

A. Network Description Matrices

The set of network description matrices, which is defined as the algorithm's input, comprises information about the network's topology and its termination loading. Consider a network with m termination points T_i for $i \in [1, m]$ and n internal nodes C_j, for $j \in [1, n]$, which is described by the following matrices:

1) $\mathbf{TC}[\mathrm{m}\times\mathrm{n}]$, which describes the interconnections between termination points and internal nodes. Each line corresponds to a termination point T_i and each column to a node C_j:

$$\mathbf{TC} = \begin{bmatrix} tc_{11} & tc_{12} & \cdots & tc_{1n} \\ tc_{21} & tc_{22} & \cdots & tc_{2n} \\ \vdots & \vdots & \ddots & \vdots \\ tc_{m1} & tc_{m2} & \cdots & tc_{mn} \end{bmatrix} \tag{8}$$

where

$$tc_{ij} = \begin{cases} 1, & \text{when } \exists\, T_iC_j \text{ connection } \forall i,j \\ 0, & \text{otherwise.} \end{cases}$$

2) $\mathbf{CC}[\mathrm{n}\times\mathrm{n}]$, which describes the interconnections between the internal nodes. Each line and each column correspond to a certain node C_i. Since $C_iC_j = C_jC_i$ and nodes cannot be connected to themselves ($C_iC_i = 0$), the $\mathbf{CC}$ matrix has zero diagonal, and exhibits symmetry around it

$$\mathbf{CC} = \begin{bmatrix} 0 & cc_{12} & \cdots & cc_{1n} \\ cc_{21} & 0 & \cdots & cc_{2n} \\ \vdots & \vdots & \ddots & \vdots \\ cc_{n1} & cc_{n2} & \cdots & 0 \end{bmatrix} \tag{9}$$

where

$$cc_{ij} = \begin{cases} 1, & \text{when } \exists\, C_iC_j \text{ connection } \forall i,j \\ 0, & \text{otherwise.} \end{cases}$$

3) $\mathbf{LT}[\mathrm{m}\times\mathrm{n}]$, which is generated by replacing the nonzero elements of $\mathbf{TC}$ matrix with the corresponding lengths $l_{T_iC_j}$

$$\mathbf{LT} = \begin{bmatrix} lt_{11} & lt_{12} & \cdots & lt_{1n} \\ lt_{21} & lt_{22} & \cdots & lt_{2n} \\ \vdots & \vdots & \ddots & \vdots \\ lt_{m1} & lt_{m2} & \cdots & lt_{mn} \end{bmatrix} \tag{10}$$

where

$$lt_{ij} = \begin{cases} l_{T_iC_j}, & \text{when } \exists\, T_iC_j \text{ connection } \forall i,j \\ 0, & \text{otherwise.} \end{cases}$$

4) $\mathbf{LC}[\mathrm{n}\times\mathrm{n}]$, which is generated by replacing the nonzero elements of $\mathbf{CC}$ matrix with the corresponding lengths $l_{C_iC_j}$. The $\mathbf{LC}$ is also symmetric around its zero diagonal

$$\mathbf{LC} = \begin{bmatrix} 0 & lc_{12} & \cdots & lc_{1n} \\ lc_{21} & 0 & \cdots & lc_{2n} \\ \vdots & \vdots & \ddots & \vdots \\ lc_{n1} & lc_{n2} & \cdots & 0 \end{bmatrix} \tag{11}$$

where

$$lc_{ij} = \begin{cases} l_{C_iC_j}, & \text{when } \exists\, C_iC_j \text{ connection } \forall i,j \\ 0, & \text{otherwise.} \end{cases}$$

5) $\mathbf{ZT}[1\times\mathrm{m}]$, which determines the impedances connected to every termination point

$$\mathbf{ZT} = [Z_{T_1} \quad Z_{T_2} \quad \cdots \quad Z_{T_m}]. \tag{12}$$

Using the above network description matrices, any indoor power-line network can be described. Additionally, the calculation procedure requires the transmission properties of the specific cable type used for the wiring. The characteristic impedance Z_0 and the propagation constant γ of each cable can be measured or calculated through transmission-line theory equations, using the cable's primary parameters (R', L', C', G') [6]. Although the presented algorithm focuses on homogeneous networks that consist of a single type of cable, it can be extended to support multiple cable types in different network sections.

B. Calculation of Network Reflection Coefficients

The algorithm presented in this paragraph calculates the reflection and transmission coefficients at each network discontinuity, namely, termination points and internal nodes. The reflection coefficients are calculated using (1), where Z_L is the

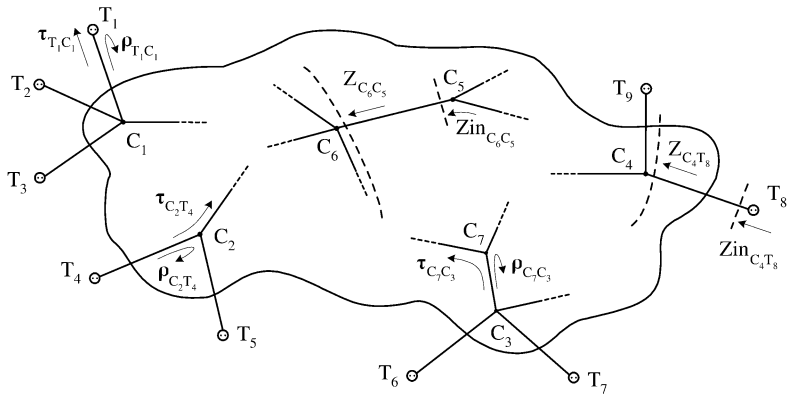

Fig. 2. Impedances, reflection, and transmission coefficients on a power-line network.

total impedance appearing to be connected to the specific network point or node for a signal traveling toward it. Throughout this text, we use index notations to indicate the direction of signal propagation (e.g., the term T_iC_j indicates propagation from node C_j toward point T_i), while Fig. 2 can be used as a reference. We define three categories of reflection coefficients based on the direction of the travelling signal, comprising the following reflection coefficient matrices:

1) $\boldsymbol{\rho}_{\mathbf{TC}}[\mathrm{m} \times \mathrm{n}]$, whose element $\rho_{TC}(i,j)$ expresses the reflection coefficient for a signal traveling from internal node C_j to the adjacent termination point T_i. In this case, Z_L in (1) is equal to the termination impedance Z_{T_i}. Therefore, for each of the m termination points, we calculate ρ_{T_i} as

$$\rho_{T_i} = \frac{Z_{T_i} - Z_0}{Z_{T_i} + Z_0}, \quad \forall i \in [1, m]. \tag{13}$$

We define the matrix $\mathbf{D}\boldsymbol{\rho}_{\mathbf{T}}[\mathrm{m} \times \mathrm{m}]$ using the above m values as its diagonal elements

$$\mathbf{D}\boldsymbol{\rho}_{\mathbf{T}} = \begin{bmatrix} \rho_{T_1} & 0 & \cdots & 0 \\ 0 & \rho_{T_2} & \cdots & 0 \\ \vdots & \vdots & \ddots & \vdots \\ 0 & 0 & \cdots & \rho_{T_m} \end{bmatrix}. \tag{14}$$

Matrix $\boldsymbol{\rho}_{\mathbf{TC}}$ is then calculated as

$$\boldsymbol{\rho}_{\mathbf{TC}} = \mathbf{D}\boldsymbol{\rho}_{\mathbf{T}} \cdot \mathbf{TC}. \tag{15}$$

2) $\boldsymbol{\rho}_{\mathbf{CC}}[\mathrm{n} \times \mathrm{n}]$, whose element $\rho_{CC}(i,j)$ expresses the reflection coefficient on node C_i for a signal travelling from internal node C_j to C_i. In this case, Z_L is equal to the aggregate impedance that appears at node $C_i(Z_{C_iCj})$, resulting from the parallel connection of the characteristic impedances of every cable that branches from that node, except for the cable on which the arriving signal is propagating. In a homogeneous network, for a node C_i connected to s_i adjacent nodes or points, s_i and Z_{C_iCj} are calculated using the following expressions:

$$s_i = \sum_{k=1}^{m} TC(k,i) + \sum_{k=1}^{n} CC(k,i) \tag{16}$$

$$Z_{C_iCj} = \frac{Z_0}{s_i - 1}. \tag{17}$$

Since the same impedance appears to a signal propagating on any of the s_i branches toward node $C_i\,(Z_{C_i} = Z_{C_iCj}\ \forall j\ \exists\ C_iC_j$ connection), we calculate n different values of Z_{C_i}: one for each of the n internal nodes. Using $Z_L = Z_{C_i}$ in (1), we calculate n reflection coefficients for the respective nodes according to

$$\rho_{C_i} = \frac{2 - s_i}{s_i}. \tag{18}$$

The calculated reflection coefficients are used as the diagonal elements of matrix $\mathbf{D}\boldsymbol{\rho}_{\mathbf{C}}[\mathrm{n} \times \mathrm{n}]$

$$\mathbf{D}\boldsymbol{\rho}_{\mathbf{C}} = \begin{bmatrix} \rho_{C_1} & 0 & \cdots & 0 \\ 0 & \rho_{C_2} & \cdots & 0 \\ \vdots & \vdots & \ddots & \vdots \\ 0 & 0 & \cdots & \rho_{C_n} \end{bmatrix}. \tag{19}$$

Matrix $\boldsymbol{\rho}_{\mathbf{CC}}$ is then calculated using the expression

$$\boldsymbol{\rho}_{\mathbf{CC}} = \mathbf{D}\boldsymbol{\rho}_{\mathbf{C}} \cdot \mathbf{CC}. \tag{20}$$

3) $\boldsymbol{\rho}_{\mathbf{CT}}[\mathrm{n} \times \mathrm{m}]$, whose element $\rho_{CT}(i,j)$ expresses the reflection coefficient at node C_i, for a signal traveling from termination point T_j toward C_i. As in the previous case, Z_L is equal to the aggregate impedance that appears at node $C_i\,(Z_{C_iTj} = Z_{C_i})$, resulting from the parallel connection of the characteristic impedances of every cable that branches from that node, except for the cable of original propagation (C_iTj). In a homogeneous network, we calculate the $\boldsymbol{\rho}_{\mathbf{CT}}$ matrix, using the transverse $\mathbf{TC}^{\mathbf{T}}$ matrix according to the following expression:

$$\boldsymbol{\rho}_{\mathbf{CT}} = \mathbf{D}\boldsymbol{\rho}_{\mathbf{C}} \cdot \mathbf{TC}^{\mathbf{T}}. \tag{21}$$

The resulting reflection coefficient matrices maintain the form and properties of the generating matrices ($\mathbf{TC}$, $\mathbf{CC}$, and $\mathbf{CT} = \mathbf{TC}^{\mathbf{T}}$, respectively). In a nonhomogeneous network, the above calculations have to be performed for each element individually, since the impedance equality at nodes (independent of propagation direction) is no longer valid. The calculated elements correspond to the nonzero elements of the generating matrices. Finally, using (1), we also calculate the respective transmission coefficient matrices ($\boldsymbol{\tau}_{\mathbf{TC}}, \boldsymbol{\tau}_{\mathbf{CC}}$, and $\boldsymbol{\tau}_{\mathbf{CT}}$).

C. Calculation of Network Input Impedances

In order to estimate the transfer function of any point-to-point channel on the network using (7), the input impedances appearing at every termination point have to be determined. As these impedances represent the aggregate impedance appearing at the input point at steady state, the calculation procedure requires the estimation of the equivalent impedances at every network point. Throughout this text, we used the following naming conventions as shown in Fig. 2.

1) $Z_{(C \text{ or } T)_i(C \text{ or } T)_j}$ is the equivalent impedance at node or point with index i for a signal traveling toward it from node or point with index j.
2) $Z_{\text{in}_{(C \text{ or } T)_i(C \text{ or } T)_j}}$ is the input impedance of the line section that connects the nodes or points with indices i and j when entering the section at node or point with index j.

The input impedance of a line section terminated by Z_L is given by

$$Z_{\text{in}} = Z_0 \cdot \frac{Z_L + Z_0 \cdot \tanh(\gamma \cdot l)}{Z_L + Z_0 \cdot \coth(\gamma \cdot l)} \tag{22}$$

where l is the section length. The following steps describe the process used in order to calculate the network impedances:

- *Step 1*: The process begins by calculating the input impedance matrix $\mathbf{Z_{in_{TC}}}[\text{m} \times \text{n}]$. Its elements $Z_{\text{in}_{TC}}(i,j)$ are calculated using (22) with $Z_L = Z_{T_i}\ \forall i \in [1,m]$ and the corresponding length $l_{T_iC_j}$ as follows:

$$Z_{\text{in}_{TC}}(i,j) = Z_0 \cdot \frac{Z_{T_i} + Z_0 \cdot \tanh(\gamma \cdot l_{T_iC_j})}{Z_{T_i} + Z_0 \cdot \coth(\gamma \cdot l_{T_iC_j})}. \tag{23}$$

  These m impedance values form a diagonal $\mathbf{DZ_{in_{TC}}}[\text{m} \times \text{m}]$ matrix, which is used to generate the requested $\mathbf{Z_{in_{TC}}}$ matrix, that maintains the form and properties of the $\mathbf{TC}$ matrix, according to

$$\mathbf{Z_{in_{TC}}} = \mathbf{DZ_{in_{TC}}} \cdot \mathbf{TC}. \tag{24}$$

- *Step 2*: The process continues with the calculation of the input and the equivalent impedance matrices of the internal nodes $\mathbf{Z_{in_{CC}}}[\text{n} \times \text{n}]$ and $\mathbf{Z_{CC}}[\text{n} \times \text{n}]$, respectively. Both matrices maintain the form of the generating $\mathbf{CC}$ matrix, but not its symmetry. Elements $Z_{\text{in}_{CC}}(i,j)$ are calculated using (22), with $Z_L = Z_{C_iC_j} \forall i,j \in [1,n]$ and the corresponding lengths $l_{C_iC_j}$ as follows:

$$Z_{\text{in}_{CC}}(i,j) = Z_0 \cdot \frac{Z_{C_iC_j} + Z_0 \cdot \tanh(\gamma \cdot l_{C_iC_j})}{Z_{C_iC_j} + Z_0 \cdot \coth(\gamma \cdot l_{C_iC_j})}. \tag{25}$$

  Equivalent impedance matrix $\mathbf{Z_{CC}}$ is formed by elements $Z_{CC}(i,j)$, as the result of the parallel connection of all input impedances, as they appear to a signal traveling from C_i toward every adjacent point or node, except C_j:

$$Z_{CC}(i,j) = /\!/\!/\left(\underbrace{Z_{\text{in}_{TC}}(x,i)}_{\forall x \in [1,m]},\ \underbrace{Z_{\text{in}_{CC}}(y,i)}_{\forall y \neq j \in [1,n]}\right). \tag{26}$$

  Expressions (25) and (26) indicate that the calculation of Z_{CC} elements require $Z_{\text{in}_{CC}}$ elements and vice versa. Therefore, calculation of the two matrices has to be performed simultaneously. Since all required elements are not *a priori* known, a computationally efficient process was developed in order to determine the next element that can be calculated using those already available. A detailed description of this process is given in the Appendix.

- *Step 3*: This step involves calculation of the equivalent impedance matrix $\mathbf{Z_{in_{CT}}}[\text{n} \times \text{m}]$. We begin by calculating the m values of $Z_{C_iT_j} \forall j \in [1,m]$ using the matrices calculated in the previous steps

$$Z_{CT}(i,j) = /\!/\!/\left(\underbrace{Z_{\text{in}_{TC}}(x,i)}_{\forall x \neq j \in [1,m]},\ \underbrace{Z_{\text{in}_{CC}}(y,i)}_{\forall y \in [1,n]}\right). \tag{27}$$

  Using the m Z_{CT} values, we calculate $Z_{\text{in}_{CT}}(i,j)$ by replacing Z_L with $Z_{C_iT_j}$ and l with $l_{T_iC_j}$ in (22) as follows:

$$Z_{\text{in}_{CT}}(i,j) = Z_0 \cdot \frac{Z_{C_iT_j} + Z_0 \cdot \tanh(\gamma \cdot l_{T_iC_j})}{Z_{C_iT_j} + Z_0 \cdot \coth(\gamma \cdot l_{T_iC_j})}. \tag{28}$$

  These m impedance values form a diagonal matrix $(\mathbf{DZ_{in_{CT}}}[\text{m} \times \text{m}])$ that is used to generate the requested $\mathbf{Z_{in_{CT}}}$, which maintains the form and properties of the $\mathbf{TC^T}$ matrix, according to

$$\mathbf{Z_{in_{CT}}} = \mathbf{TC^T} \cdot \mathbf{DZ_{in_{CT}}}. \tag{29}$$

Having calculated the input impedances appearing at steady state for a signal propagating from any termination point toward any adjacent node, along with the network reflection and transmission coefficients, we can proceed with the calculation of the multipath components and the channel's transfer function.

D. Analytical Calculation of Multipath Components

Using the calculated values of every network reflection and transmission coefficient, we proceed with the estimation of the factors that comprise each of the multipath components received on a certain point-to-point channel. It should be noted that since Z_0 and γ are frequency-dependent variables, the propagation loss factors, the reflection and transmission coefficients also vary with frequency. Therefore, the previously described calculation steps refer to a particular frequency and are repeated with a properly selected frequency step to represent the entire frequency band of interest. As a result, every calculated parameter is, in fact, a vector of N values, where N is the number of subchannels into which the frequency band has been divided. Throughout this text, the discussion regards frequency-dependent parameters, with values calculated using the subchannel center frequencies.

Calculation of the reflection and propagation factors in (6) requires a large number of paths $L_{\max}$. However, only L of these paths make a nontrivial contribution to the overall channel response and are regarded as significant paths. This selection is based on the following component power criterion. We initially consider the total signal power, calculated using a very large number of paths $(L_{\max})$ and select the first L paths to reach the receiver as significant, when their aggregate power is at least

equal to a predefined threshold level (e.g., 96%) [2] when compared to the total power

$$\frac{\sum_{i=1}^{L}|h_i|^2}{\sum_{i=1}^{L_{\max}}|h_i|^2} \geq 0.96 \tag{30}$$

where h_i is the multipath component that corresponds to the ith path, and $|h_i|^2$ is its power magnitude.

The process continues with the calculation of the channel's transfer function according to (7), using the computed values of the steady-state input impedances of the network. As an example of how each multipath component is computed, we describe two typical paths on the simple network, shown in Fig. 3. According to (4), the reflection factor of each path is equal to the product of all the coefficients that comprise it. Thus, for path 1 $(T_1 - C_1 - T_4)$ and path 2 $(T_1 - C_1 - C_2 - C_1 - T_4)$, the reflection factors and the respective path lengths are given by

$$\begin{aligned} r_1 e^{j\theta_1} &= \tau_{C_1T_1} \cdot \tau_{T_4C_1} \\ l_1 &= l_{C_1T_1} + l_{T_4C_1} \\ r_2 e^{j\theta_2} &= \tau_{C_1T_1} \cdot \rho_{C_2C_1} \cdot \tau_{C_1C_2} \cdot \tau_{T_4C_1} \\ l_2 &= l_{C_1T_1} + 2 \cdot l_{C_2C_1} + l_{T_4C_1}. \end{aligned} \tag{31}$$

It should be noted that these paths are not consecutive in the order of arrival at the receiver end. Lengths l_1 and l_2 are used to calculate the propagation factor $\left(e^{-\gamma l_i} = e^{-\alpha l_i} \cdot e^{-j\omega\tau_{di}}\right)$ of each path, expressing the effect of propagation on the cable, in terms of amplitude and phase. Thus, the multipath components corresponding to these particular transmission paths can be calculated. The sum of all components, calculated for the significant paths between the specified transmitter–receiver pair, determines the channel response. Consequently, using the input impedance that corresponds to the input termination point $(Z_{\text{in}_{C_1T_1}})$, we determine the transfer function of the communications channel from point T_1 to T_4.

Finally, we should also comment on the symmetry of the two opposite transmission directions on any power-line channel. Generally, the structure of the power grid does not allow for symmetry on the communications channels it comprises. Nevertheless, certain conditions, which are commonly valid in the indoor environment, lead to an acceptable channel symmetry assumption. Specifically, it has been proven that symmetry on power-line channels exists when the impedances connected to the two communicating end points are identical [7]. In the indoor environment, electrical loads can be divided into two categories: loads with impedances significantly lower than the characteristic impedance of the cable (Z_0) (e.g., heating devices, refrigerators, ovens, clothes dryers), which do not require high-speed data communications, and loads that exhibit impedances much higher than Z_0, such as digital data or multimedia devices and which are probable candidates for high-speed data transmission. The power supply of such devices is connected in parallel to the power-line transceiver and its effect on the total termination impedance is negligible since transceivers are designed to have impedances close to Z_0, while the power supplies exhibit much larger impedances. Therefore, under such communications conditions, it is valid to state that each point-to-point connection that complies with the above assumption can be characterized as symmetric.

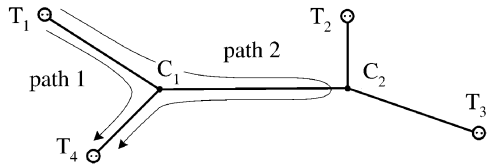

Fig. 3. Example of two propagation paths.

IV. Example of Multipath Components Calculation

The performance of power-line communications systems is determined by a number of parameters, such as noise, signal attenuation, frequency and time spreading. Extensive characterization of the sources of disturbance in the power-line environment can be found in the literature [5], [8]. In this work, we focus on describing the effect of signal distortion due to propagation in the network. As was already mentioned, the power-line channel can be characterized as a multipath fading environment with time- and frequency-varying behavior. Time variations in its termination loading, namely, loads (e.g., electrical appliances) being connected to or disconnected from the network, or even altering their impedance during normal operation, cause its impulse response to vary. The channel, however, appears to be changing rather slowly (at least every few milliseconds) compared to the symbol duration in high-speed data communications. On the other hand, multipath propagation results in time spreading of the transmitted signal, which is expressed by the mean delay (τ_{avg}) and the root mean square (rms) delay spread (σ_τ), according to

$$\tau_{\text{avg}} = \frac{\sum_{i=1}^{L}\{\tau_{di}|h_i|^2\}}{\sum_{i=1}^{L}\{|h_i|^2\}} \quad \text{and}$$
$$\sigma_\tau = \sqrt{\frac{\sum_{i=1}^{L}\{(\tau_{di}-\tau_{\text{avg}})^2|h_i|^2\}}{\sum_{i=1}^{L}\{|h_i|^2\}}}. \tag{32}$$

The reciprocal of the rms delay spread is used to determine the coherence bandwidth of the channel $(\Delta f)_c$, which is defined as the range of frequencies for which the channel displays frequency-nonselective characteristics $(\Delta f)_c \ll (1/\sigma_\tau)$. Equivalently, if the signaling interval (T_s) is selected to be $T_s \gg \sigma_\tau$, the channel introduces negligible intersymbol interference.

The algorithm presented in this paper can be utilized to calculate parameters such as rms delay spread, optimum subchannel bandwidth, and suitability of each subchannel for data transmission parameters, which are necessary in order to configure such a system with regards to the data transmission rate over the channel and the allocation of bandwidth for reliable communications.

Consider the power-line topology presented in Fig. 4. We use the multipath components' calculation algorithm to estimate the

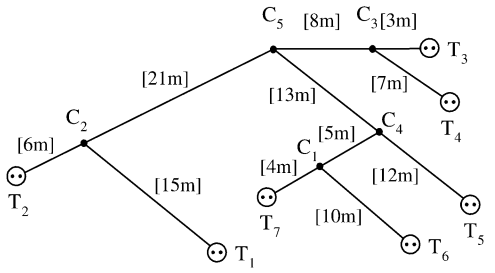

Fig. 4. Indoor power-line network example.

relationship between different communications parameters. The network description matrices used as the algorithm's input are

$$\mathbf{TC}=\begin{bmatrix}0&1&0&0&0\\0&1&0&0&0\\0&0&1&0&0\\0&0&1&0&0\\0&0&0&1&0\\1&0&0&0&0\\1&0&0&0&0\end{bmatrix}\quad \mathbf{LT}=\begin{bmatrix}0&15&0&0&0\\0&6&0&0&0\\0&0&3&0&0\\0&0&7&0&0\\0&0&0&12&0\\10&0&0&0&0\\4&0&0&0&0\end{bmatrix}$$

$$\mathbf{CC}=\begin{bmatrix}0&0&0&1&0\\0&0&0&0&1\\0&0&0&0&1\\1&0&0&0&1\\0&1&1&1&0\end{bmatrix}\quad \mathbf{LC}=\begin{bmatrix}0&0&0&5&0\\0&0&0&0&21\\0&0&0&0&8\\5&0&0&0&13\\0&21&8&13&0\end{bmatrix}.$$

We assume that there are three communicating devices on the network, connected to termination points T_1, T_2, and T_5. The total impedance of each device is 100 Ω, including the impedances of the transceiver and the power supply of the communicating device. Regarding the remaining termination points on the network (T_3, T_4, T_6, and T_7), three loading cases (l.c.) have been considered, each corresponding to a different $\mathbf{ZT}$ matrix. The first loading case regards the remaining points as being unloaded (open circuits), the second considers different impedances connected to each termination point, and the third assumes that a communications device is connected to every termination. It is assumed that the connection of the indoor power-line network to the external power grid is performed using a high-current lowpass filter that does not change its impedance as time progresses and, therefore, it has been omitted from this qualitative analysis. The $\mathbf{ZT}$ matrices corresponding to these loading conditions are the following:

$$\mathbf{ZT_{l.c.1}}=[100\quad 100\quad 10^8\quad 10^8\quad 100\quad 10^8\quad 10^8]$$
$$\mathbf{ZT_{l.c.2}}=[100\quad 100\quad 50\quad 8\quad 100\quad Z_0/4\quad 75]$$
$$\mathbf{ZT_{l.c.3}}=[100\quad 100\quad 100\quad 100\quad 100\quad 100\quad 100].$$

Some of the above loading conditions might represent extreme cases of network loading, but they were selected in order to display the potentials of the calculation procedure. In our calculations, the open-circuit condition is represented as an impedance of 10^8 Ω.

As it was already described in the previous section, the frequency band of interest is divided into N subchannels and the calculation steps of the algorithm are repeated for each subchannel using its center frequency. Initially, we determine the order of the specific power-line channel, which is equivalent to the selection of the L most significant transmission paths. Using the component power criterion, we determine the finite duration

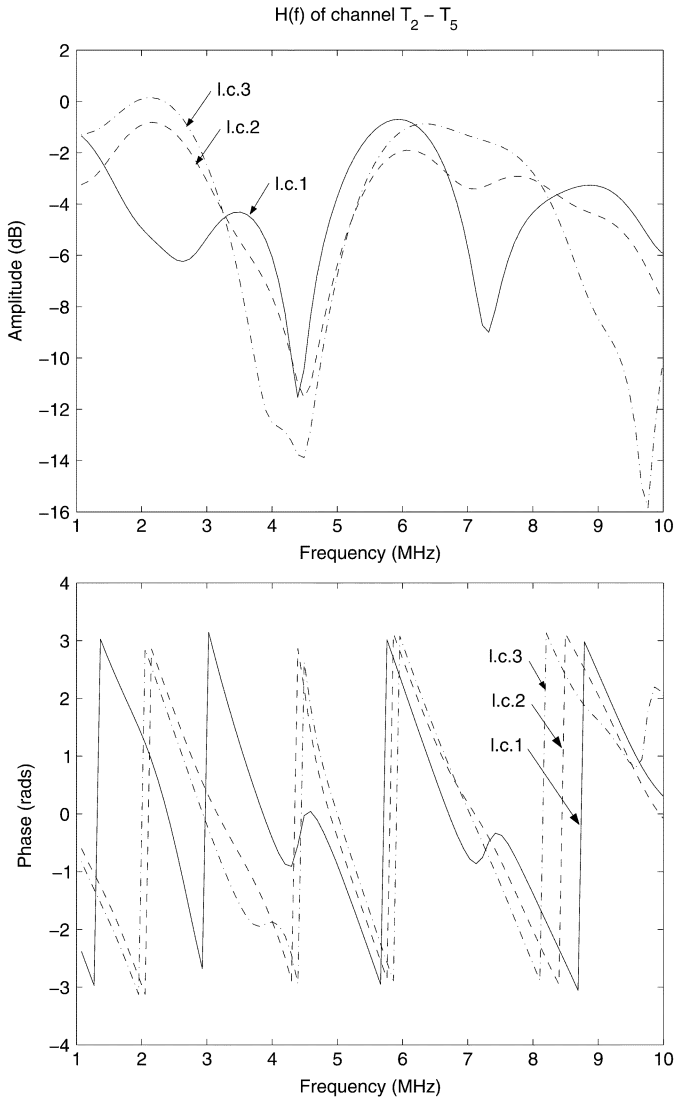

Fig. 5. Frequency response of channel $T_2 - T_5$ in the 1–10-MHz band.

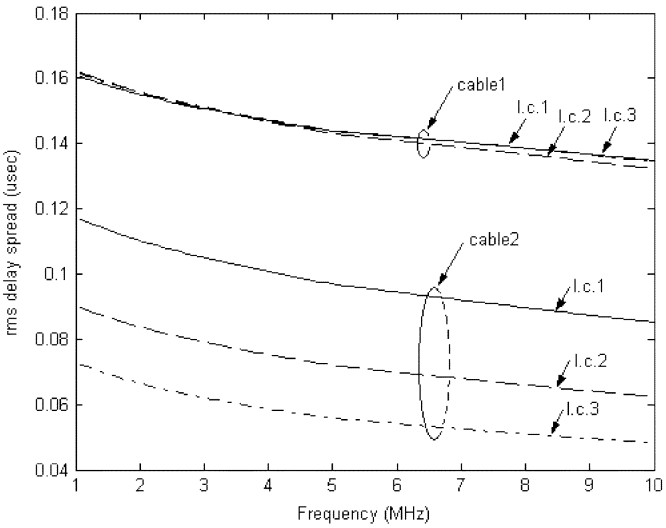

Fig. 6. RMS delay spread for channel $T_2 - T_5$ with two types of cables and three loading conditions.

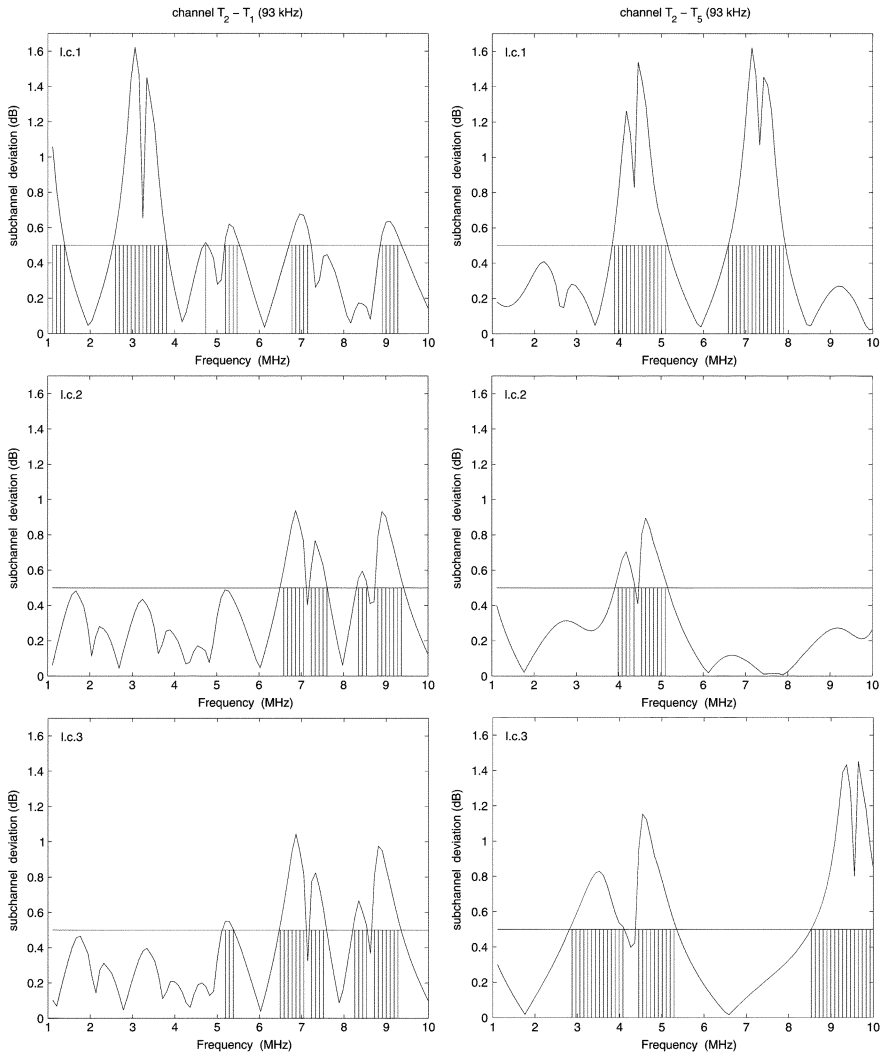

Fig. 7. Maximum deviation of power magnitude response of channels $T_2 - T_5$ and $T_2 - T_1$ with nonflat subchannels marked.

of the channel's impulse response (L). This implies that the impulse response is assumed to decay fast enough, so that beyond the Lth arriving component, the contribution to the overall received signal power becomes insignificant. The frequency response of the transmission channel from point T_2 to T_5, calculated for a power threshold of 96% and using all three loading conditions is shown in Fig. 5. This figure demonstrates the effect of varying loading conditions on the channel's frequency response. As the loading conditions change, the channel may experience deep fading conditions that make some subchannels unsuitable for data transmission.

The channel's rms delay spread as a function of frequency is presented in Fig. 6 for two different types of cables described in [6] (cable1) and [9] (cable2). Cable1 is the type used for all other results demonstrated in this section. It can be concluded that the rms delay spread strongly depends on the cable's characteristics. Additionally, we observe that the effect of the varying loading conditions also depends on the cable's type.

The presented algorithm can also be used to determine the optimum subchannel bandwidth $\mathrm{BW_{sub}}$ that has to be selected so that the channel response is considered constant within the corresponding frequency range. In this respect, the channel appears as frequency nonselective for any transmitted signal with bandwidth $B_s \leq \mathrm{BW_{sub}}$. Considering different levels of power magnitude deviation, the calculated optimum $\mathrm{BW_{sub}}$ on the $T_2 - T_5$ channel for all three loading conditions is shown in Table I.

TABLE I
OPTIMUM SUBCHANNEL BANDWIDTH

Maximum Power Deviation [dB]	Bandwidth [kHz]
0.5	19.5
1.0	48.8
1.5	83.0
2.0	117.2
2.5	151.4
3.0	180.6

Moreover, given a certain $\mathrm{BW_{sub}}$ and a predefined deviation threshold in the channel response, we can estimate the number of efficient subchannels regarding the flatness of their response. In Fig. 7, we present the maximum power magnitude deviation for $\mathrm{BW_{sub}} \cong 93$ kHz and we mark the inefficient (nonflat) subchannels, according to the 0.5-dB deviation threshold. The subfigures on the left correspond to the $T_2 - T_1$ channel, while the

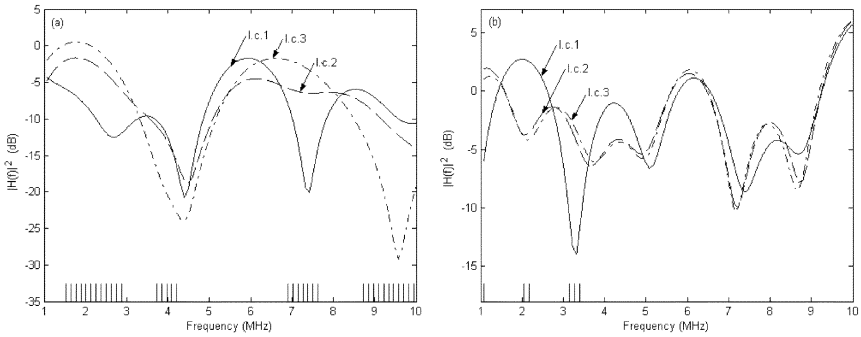

Fig. 8. Squared transfer function and unsuitable subchannels (marked) under various network loading conditions for channels (a) $T_2 - T_5$ and (b) $T_2 - T_1$.

ones on the right correspond to the $T_2 - T_5$ channel. Each row of subfigures represents a different loading condition.

Using the calculated frequency response, we can also estimate which subchannels exhibit power magnitude characteristics, which are bounded within a certain deviation threshold (e.g., 6 dB), under any loading condition. This estimation is presented in Fig. 8 for the two transmission channels [(a) $T_2 - T_5$ and (b) $T_2 - T_1$], the three loading conditions, and $\mathrm{BW_{sub}} \cong 25$ kHz, where the marked subchannels exhibit power magnitude characteristics that are severely (over 6 dB) affected by changes in network loading. It can be deduced that using the presented algorithm, we can determine suitable frequency bands under various loading conditions for each channel and combining these results we can proceed to allocate the appropriate bandwidth to the various communications channels on the network. This procedure can be applied to any frequency band of interest, while the 1–10-MHz band was selected here for reasons of clarity in the presented figures.

V. Conclusion

This paper presented an analytic algorithm that facilitates efficient calculation of the multipath effect in indoor power-line networks, based on their physical characteristics and termination loading. The algorithm can be used for determining the quality of transmission between any pair of communicating devices on a power-line network and for performing optimization on the available resources.

It has been established that by estimating the multipath signal components on a transmission channel, a number of important communications parameters can be derived, such as rms delay spread and characterization of the efficiency of its subchannels based on their frequency selectivity and their sensitivity to loading variations. The presented methodology can also be used to derive a general power-line communications model, describing the channel's transmission behavior in terms of network physical structure and loading conditions.

Appendix
Concurrent Computation of the Impedance Matrices

In Subsection III–C, we concluded that the $\mathbf{Z_{in_{CC}}}$ and $\mathbf{Z_{CC}}$ impedance matrices have to be computed simultaneously, since all required elements are not known prior to calculation. The process proposed in this Appendix estimates the next element that can be calculated from those already available and has to be used in order to avoid unnecessary or unsolvable impedance calculation steps. The process is based on the rearrangement of the $\mathbf{TC}, \mathbf{CC}$, and all corresponding matrices, which facilitates an element calculation sequence that involves only elements that have already been calculated. This becomes feasible when the process begins with nodes closer to the termination points, regarded as "outer nodes," and proceeds with those further toward the network core, regarded as "inner" nodes. The rearrangement procedure is performed according to the following rule:

The smallest indices of the new $\mathbf{CC}$ matrix correspond to "outer" nodes, whereas the largest indices correspond to "inner" nodes. The criterion of characterizing a node is based on its proximity to all other nodes and termination points on the network.

In order to give a detailed description of the nodes' rearrangement and the concurrent matrix calculation process, we define an adjacency matrix $\mathbf{A}[(\mathrm{m}+\mathrm{n}) \times (\mathrm{m}+\mathrm{n})]$

$$\mathbf{A}_{[(m+n)\times(m+n)]} = \begin{bmatrix} 0_{[m\times m]} & TC_{[m\times n]} \\ TC^{T}_{[n\times m]} & CC_{[n\times n]} \end{bmatrix}. \tag{33}$$

The adjacency matrix describes the connections between any node or termination point on the network. According to [10], the power of the adjacency matrix has an important property: element $\mathbf{A}^k(i,j)$ expresses the number of different itineraries, containing k line sections, between the two points or nodes that correspond to the row and column indices (i and j).

In this respect, the node with the largest sum of elements of the kth power is the node most frequently reached from the others, namely the most central node, when k line sections are taken under consideration. As a result, if we consider the sum of every power of $\mathbf{A}$ up to the Kth, we can sort the nodes based on the sum of the corresponding columns. This rearrangement orders the nodes sequentially from the most "inner" to the most "outer" node. Specifically, we define D_j as the sum of C_j node's itineraries from any other point or node on the network

$$D_j = \sum_{i=1}^{m+n} \left\{ \sum_{k=1}^{K} A^k(i,j) \right\}. \tag{34}$$

The above procedure can be simplified by excluding the nodes that are, by definition, the most "outer." These nodes are connected to a single node and a number of termination points. The elements needed to calculate Z_{CC} and $Z_{\mathrm{in}_{CC}}$ with direction toward these nodes from their adjacent ones are related only to the termination points and have already been

determined in previous steps. Therefore, we characterize these nodes as the most "outer" ones and assign them the smallest indices (regardless of the order between them). The remaining nodes have to be assigned a new index according to the above procedure.

The power K, where the calculation procedure stops, is determined as the consecutive powers of $\mathbf{A}$ are calculated. The Kth power is the last to be derived, when there is at least one itinerary between every pair of termination points, expressed as follows:

$$\sum_{n=1}^{K} A^n(i,j) \geq 1, \quad \forall i,j \in [1,m]. \tag{35}$$

This rearrangement of the nodes gives $\mathbf{CC}$ a new significant property, while its symmetry across the zero diagonal is maintained. Keeping the naming convention that considers the column node as the node of departure and the row node as the destination, it can be concluded that elements above diagonal $(i < j)$ indicate direction from "inner to outer" nodes, whereas elements beneath diagonal $(i > j)$ indicate direction from "outer to inner" nodes. It can easily be shown that if C_i is an "outer" node compared to $C_j, Z_{C_iC_j}$ is the equivalent impedance resulting from the parallel connection of all input impedances appearing at node C_i toward the "outer" direction, which means that elements above the diagonal require only elements located above it as well. Furthermore, it is valid to consider that each node can be connected to a number of more "outer" nodes (elements above the diagonal) but only to one more "inner" node (element beneath the diagonal), meaning that there is only one nonzero element per column beneath the diagonal. By symmetry, only one nonzero element per line is located above the diagonal.

Therefore, $\mathbf{Z_{CC}}$ and $\mathbf{Z_{in_{CC}}}$ matrices can be computed using (25) and (26) in the most efficient manner:

1) The process begins with the calculation of each line of the matrices above the diagonal, beginning with the first line. Calculation of the single nonzero element of the ith line requires all of the elements of column i of $\mathbf{Z_{in_{TC}}}$, which have already been calculated, and the elements of column i of $\mathbf{Z_{in_{CC}}}$, except the one on line j. Since the direction is "from inner to outer" $(i < j)$, all needed elements $Z_{\mathrm{in}C_wC_i}$ have $w \in [1, i-1]$, because they are located above the diagonal in column i and have been calculated in previous iterations.
2) The process continues with the calculation of each column of the matrices beneath the diagonal, beginning with column $j = n-1$ and repeating until column $j = 1$. For the calculation of the only nonzero element in column $j(Z_{C_iC_j})$, the required elements $Z_{\mathrm{in}C_wC_i}$ lie in column $i \forall w \neq j$. Since $i > j$ beneath the diagonal, i refers to columns whose elements have already been determined.

REFERENCES

[1] N. Pavlidou, A. J. H. Vinck, J. Yazdani, and B. Honary, "Power line communications: State of the art and future trends," *IEEE Commun. Mag.*, vol. 41, pp. 34–40, Apr. 2003.

[2] D. Liu, B. Flint, B. Gaucher, and Y. Kwark, "Wide band AC power line characterization," *IEEE Trans. Consumer Electron.*, vol. 45, pp. 1087–1097, Nov. 1999.

[3] H. Philips, "Modeling of powerline communication channels," in *Proc. Int. Symp. Power-Line Commun.*, Lancaster, U.K., 1999, pp. 14–21.

[4] M. Zimmermann and K. Dostert, "A multipath model for the powerline channel," *IEEE Trans. Commun.*, vol. 50, pp. 553–559, Apr. 2002.

[5] ——, "Analysis and modeling of impulsive noise in broad-band power-line communications," *IEEE Trans. Electromagn. Compat.*, vol. 44, pp. 249–258, Feb. 2002.

[6] S. Tsuzuki, T. Takamatsu, H. Nishio, and Y. Yamada, "An estimation method of the transfer function of indoor power-line channels for Japanese houses," in *Proc. Int. Symp. Power-Lines Commun.*, Athens, Greece, 2002, pp. 55–59.

[7] T. C. Banwell and S. Galli, "On the symmetry of the power line channel," in *Proc. Int. Symp. Power-Lines Commun.*, Malmo, Sweden, 2001, pp. 325–330.

[8] A. Voglgsang, T. Langguth, G. Korner, H. Steckenbiller, and R. Knorr, "Measurement characterization and simulation of noise on power-line channels," in *Proc. Int. Symp. Power-Lines Commun.*, Limerick, Ireland, 2000, pp. 139–146.

[9] F. Issa and A. Abdouss, "Indoor PLC network simulator," in *Proc. Int. Symp. Power-Lines Commun.*, Athens, Greece, 2002, pp. 36–39.

[10] V. K. Balakrishnan, *Schaum's Outline of Theory and Problems of Graph Theory*. New York: McGraw-Hill, 1997.

Despina Anastasiadou was born in Thessaloniki, Greece, in 1975. She received the Diploma and the Ph.D. degrees in electrical engineering from the Department of Electrical and Computer Engineering, University of Patras, Patras, Greece, in 1998 and 2004, respectively.

Since September 1998, she has been a Research Engineer with the Laboratory of Electromagnetics, participating in R&D projects supported by the Greek Government and European industries. In 2000, she joined the Computer Technology Institute, Patras. Her research interests include data communication networks with an emphasis on power-line communications, signal processing, and embedded systems design.

Ms. Anastasiadou is a member of the Technical Chamber of Greece.

Theodore Antonakopoulos (M'88–SM'99) was born in Patras, Greece, in 1962. He received the Diploma and Ph.D. degrees in electrical engineering from the Department of Electrical Engineering, University of Patras, in 1985 and 1989, respectively.

Currently, he is an Associate Professor with the Faculty of the Electrical Engineering Department, University of Patras. In September 1985, he joined the Laboratory of Electromagnetics, University of Patras, participating in various R&D projects for the Greek Government and the European Union, initially as a Research Staff Member and, subsequently, as the Senior Researcher of the Communications Group. His research interests include data-communication networks, local-area networks (LANs), and wireless networks, with an emphasis on performance analysis, efficient hardware implementation, and rapid prototyping. He has many publications in the above areas and actively participates in several R&D projects of European industries.

Dr. Antonakopoulos is a member of the Technical Chamber of Greece.